



Microstructure at friction stir lap joint interface of pure titanium and steel

Jinsun Liao^{a,*}, Naotsugu Yamamoto^a, Hong Liu^b, Kazuhiro Nakata^b

^a Kurimoto Ltd., 2-8-45 Suminoe, Osaka 559-0021, Japan

^b JWRI, Osaka University, 11-1 Mihogaoka Ibaraki, Osaka 567-0047, Japan

ARTICLE INFO

Article history:

Received 2 June 2010

Accepted 16 July 2010

Available online 22 July 2010

Keywords:

Friction stir welding

Dissimilar lap joint

Intermetallic compound

Pure titanium

Transmission electron microscopy

ABSTRACT

A commercially pure titanium plate was lap joined to a structural steel plate via friction stir welding, and the microstructures at the lap joint interface were intensively examined by means of electron backscatter diffraction analysis and transmission electron microscopy. Swirling-like macro- and micro-intermixing zones of titanium and steel are formed along the interface, where tiny Fe–Ti intermetallic particles are dispersed and mixed with β titanium in layers. The lap joint has high shear tensile strength, which is supposed to result from the dispersion of tiny Fe–Ti intermetallic particles and the formation of β titanium at the joint interface.

© 2010 Elsevier B.V. All rights reserved.

1. Introduction

Titanium and its alloys have high specific strength and excellent corrosion resistance, and thus have been employed in many important industrial fields such as aerospace and chemical industries; however, wider use of these materials is limited by their expensive cost. One solution is to join titanium alloys to conventional structural steels, by which the amount of titanium alloys can be minimized so that the production cost can be reduced. There are a few works to study the dissimilar joining of titanium alloys to steels [1–5], and the key issue is to avoid the formation of brittle Fe–Ti intermetallic compounds in the joints. Diffusion bonding or friction welding, the solid-state welding process, has been generally employed since the intermixing extent of titanium and steel can be easily controlled and consequently the excessive formation of Fe–Ti intermetallic compounds is restrained [5]. While some sound joints with comparatively high tensile strength are obtained in the previous works, the joints are still the weakest region due to the existence of intermetallic compounds, and in particular the details of microstructures at the joint interface are not yet understood completely.

On the other hand, friction stir welding (FSW), a novel solid-state welding process developed by The Welding Institute (TWI), has several advantages such as a high operative efficiency and versatility as compared to the conventional solid-state welding processes. It has been successfully applied to join dissimilar metals, e.g. magnesium alloys to aluminum alloys [6–8], steels to aluminum alloys [9], whereas there is no report on FSW of titanium to steels. In the present

work, a commercially pure titanium plate was lap joined to a structural steel plate via FSW, and the microstructures at the lap joint interface were intensively investigated.

2. Experimental details

A commercially pure titanium plate (Ti-0.01C-0.03Fe-0.100-0.01N-0.001H, wt.%) with dimensions of $300 \times 100 \times 2$ mm and a structural steel plate (Fe-0.10C-0.98Mn-0.22Si-0.015P-0.003S, wt.%) with dimensions of $300 \times 100 \times 6$ mm were used in the present work. The titanium plate was lap joined to the steel plate via FSW, by placing the titanium plate on top of the steel plate, i.e. the titanium plate was in touch with the shoulder of welding tool during FSW. The welding tool for FSW was made from a sintered WC-Co based alloy and consisted of a concave shoulder with 15 mm diameter and a cylinder pin of 2 mm in length and 6 mm in diameter. Lap joining was performed via FSW at a tool rotation speed of 300 rpm and a travel speed of 75 mm min^{-1} . During FSW, water cooling system and argon shielding gas were employed to cool the welding tool and to prevent the surface oxidation of titanium plate, respectively.

After FSW, microstructure characterization of the joint was carried out on cross-sections perpendicular to the welding direction. Specimens for optical microscopy were polished and then etched with 3% Nital solution. The microstructure at the joint interface was examined in detail by means of electron backscatter diffraction (EBSD) analysis and transmission electron microscopy (TEM). Samples for EBSD were prepared using an ion polisher (JEOL SM-09010). Thin foils for TEM were prepared with a focused ion beam (FIB) instrument, and examined using a microscope (JEOL 2010) operated at 200 kV. Chemical compositions were analyzed with an energy-dispersive X-ray spectrometer equipped to the transmission electron microscope. In addition, shear

* Corresponding author. Tel.: +81 6 6686 3259 8668; fax: +81 6 6686 3149.

E-mail address: j_liao@kurimoto.co.jp (J. Liao).

tensile specimens of 20 mm in width and 155 mm in length were machined from the lap joined sample, and shear tensile test was performed at room temperature using an Instron servohydraulic load frame operating at a constant crosshead velocity of 1 mm min^{-1} .

3. Results and discussion

A low-magnification overview of the weld cross-section is presented in Fig. 1a. AS and RS are the advancing side and retreating side of the welding pool, respectively. Because the joint interface between titanium and steel plates is preferentially etched, it seems that there are cracks at the joint interface between the two plates from Fig. 1a, but the joint interface is indeed sound and the joint length without any defect is about 4 mm. Fig. 1b and c gives the scanning electron micrographs of the joint interface before etching at the locations marked in Fig. 1a. At the majority of the joint interface, titanium and steel are obviously intermixed, but the intermixing is hardly confirmed at some joint interface from the scanning electron micrographs, where the microstructures were examined in detail with TEM.

Fig. 2 shows an EBSD phase map of the microstructure at the joint interface where the intermixing between titanium and steel is obvious (e.g. the region indicated in Fig. 1b by mark I). Alpha (α) titanium (hexagonal structure) and iron (body-centered cubic structure) are given in dark color and bright color, respectively. It is clear that the swirling-like intermixing zone (i.e. macro-intermixing zone) consisting of α titanium and iron forms at the joint interface. At the macro-intermixing zone, besides α titanium and iron, there are some black regions. It is conceivable that either the grain size is too small to be distinguished by EBSD or other new phases are produced in these black regions. TEM examination reveals that the microstructures in the black regions are similar to those at the micro-intermixing zones, which are described in detail as follows.

Fig. 3a reveals a TEM micrograph of the joint interface without obvious intermixing (e.g. the region indicated in Fig. 1c by mark II). At the interfacial zone, the mean grain size of titanium and steel is ca. 150 nm and 600 nm, respectively, tremendously smaller than that of

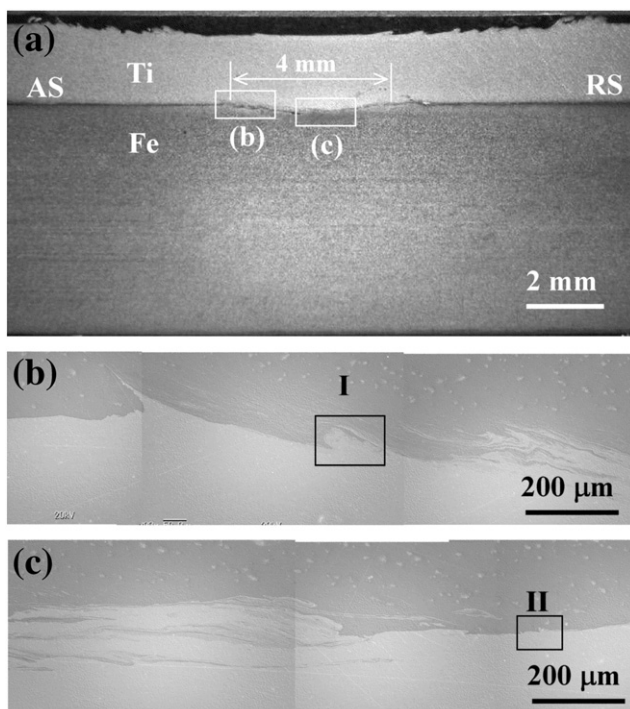


Fig. 1. Lap joint of titanium to steel via FSW: (a) low-magnification overview of the weld cross-section, (b) and (c) SEM images of the lap joint interface.

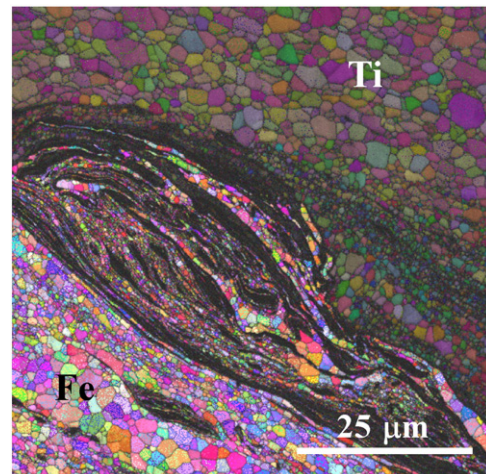


Fig. 2. EBSD phase map of the macro-intermixing zone at the joint interface.

the base metal of titanium (ca. $16 \mu\text{m}$) and steel (ca. $12 \mu\text{m}$), because they experience heavy plastic deformation and consequently dynamic recrystallization [10,11]. Between titanium and steel, there is a micro-intermixing zone of $1\text{--}2 \mu\text{m}$ in width, consisting of bright phase and dark phase. Table 1 gives the elemental analysis results at the positions from No. 1 to No. 11 in Fig. 3a. At the micro-intermixing zone, the bright phase has a high ratio of Ti (e.g. No. 4 and No. 5 positions), while the dark phase has a high ratio of Fe (e.g. No. 6 and No. 7 positions). Electron diffraction together with elemental analysis indicates that the dark phase is FeTi or Fe_2Ti intermetallic particles. A TEM micrograph of FeTi (body-centered cubic, $a = 2.976 \text{ nm}$) at the location of mark A in Fig. 3a (adjacent to No.3 position, where the atom percentage of Ti and Fe is almost identical) is presented in Fig. 3b, and its dark field image and electron diffraction pattern are given in Fig. 3c. Although the electron diffraction pattern of the bright phase at the center of the micro-intermixing zone is not obtained due to its thickness, the diffraction pattern at the boundary between the micro-intermixing zone and titanium (the location indicated by mark B in Fig. 3a) demonstrates that the bright phase of ca. 85 at.% Ti and 15 at.% Fe is β titanium (body-centered cubic, $a = 3.3065 \text{ nm}$), as shown in Fig. 3d and e. The β titanium phase and Fe–Ti intermetallic particles are also confirmed at the locations apart from the micro-intermixing zone (e.g. at the location of mark C in Fig. 3a).

It is previously reported that an intermetallic layer including FeTi and Fe_2Ti exists at the joint interface [1–5]; however, the details about the Fe–Ti intermetallic compounds are not clearly demonstrated. In the present study, swirling-like macro- and micro-intermixing zones are found at the joint interface (Figs. 2 and 3). At the macro-intermixing zones, α titanium and steel are mixed in swirling morphology; at the micro-intermixing zones, tiny Fe–Ti intermetallic particles and β titanium grains (both of them in range of ca. 100 to 200 nm) are dispersed and mixed in layers. The formation of β titanium at the joint interface is another important finding in the present study. According to the binary Fe–Ti phase diagram [12], the β transus of titanium is 863 K for the eutectic reaction between titanium and iron. While there is no temperature data measured directly at the interfacial zone during FSW, the researches on FSW of pure titanium or near- α titanium [10,13] show that the temperature at the stir zone of FSW may be higher than the β transus (ca. 1155 K) of pure titanium. Therefore, it is possible that the temperature at the joint interface in the present work is above 863 K, and β titanium transformation occurs in heating period during FSW especially at the iron-rich locations. Since the cooling rate at the stir zone and particularly the interfacial zone of dissimilar joints is tremendously high [14] and non-equilibrium phases are easily generated in FSW joint [6], β titanium phase is present at the interfacial zones as a result.

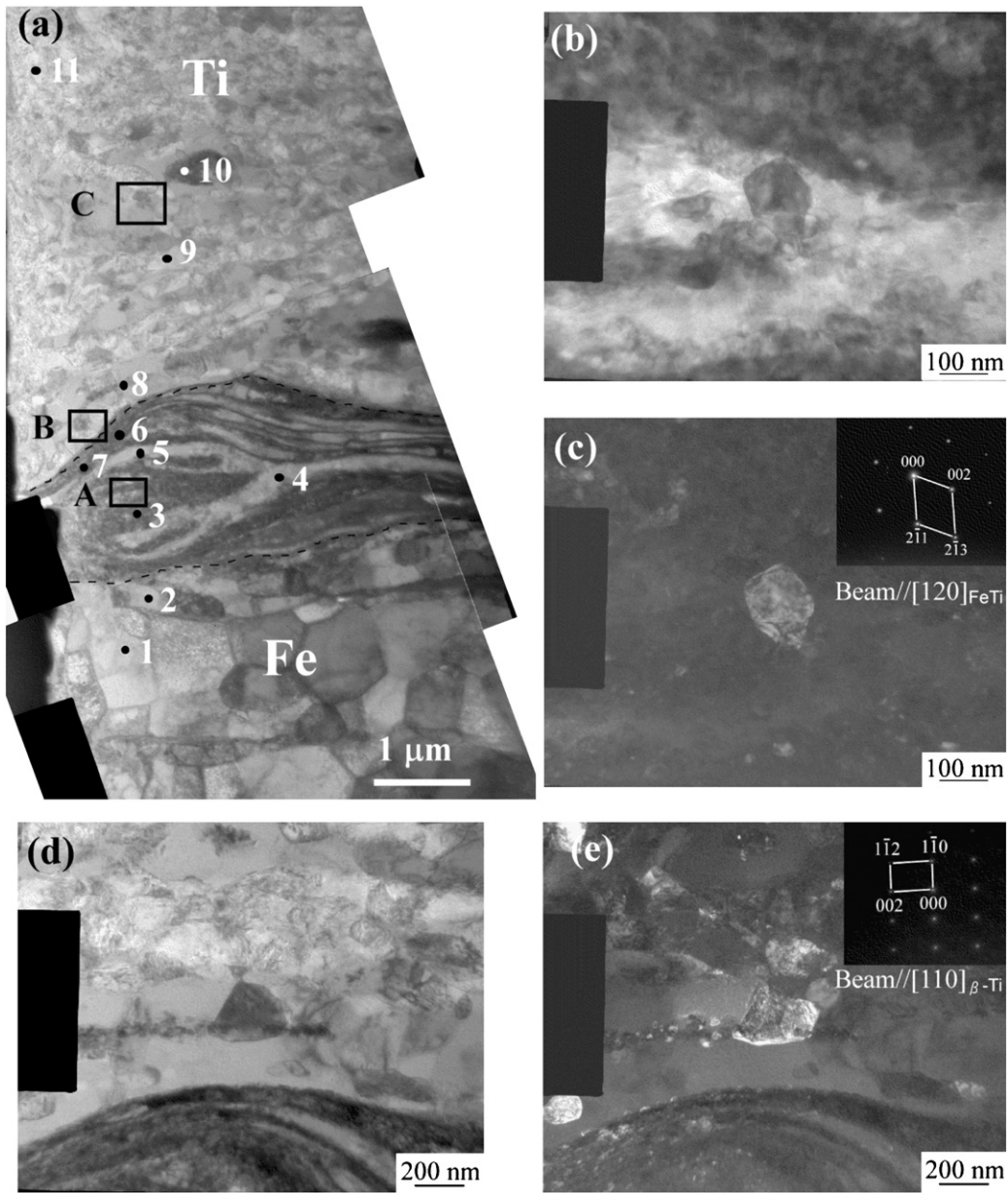


Fig. 3. TEM micrographs of the micro-intermixing zone at the joint interface: (a) overview of the micro-intermixing zone, (b) bright field image of the FeTi intermetallic compound, (c) dark field image and electron diffraction pattern of the FeTi intermetallic compound, (d) bright field image of β titanium, and (e) dark field image and electron diffraction pattern of β titanium.

Table 1
Elemental analysis results of the micro-intermixing zone.

Position	Element (at.%)				Phase
	Ti	Fe	Mn	Si	
1	0.72	98.78	0.5	–	Fe
2	3.05	95.89	1.05	–	Fe
3	52.86	46.23	0.36	0.56	FeTi
4	84.66	15.34	–	–	Ti
5	84.41	15.59	–	–	Ti
6	28.81	70.87	0.32	–	Fe ₂ Ti
7	28.82	70.87	0.31	–	Fe ₂ Ti
8	50.23	49.77	–	–	FeTi
9	98.83	1.17	–	–	Ti
10	32.37	66.43	0.63	0.57	Fe ₂ Ti
11	97.2	2.8	–	–	Ti

Shear tensile test demonstrates that the lap joint has a sufficient strength. Shear tensile specimens fracture at the titanium base metal, and the elongation of shear tensile test is very large and mainly dependent on the ductility of the pure titanium plate, as shown in Fig. 4. The average fracture load of the three specimens is 14.22 kN, suggesting that the shear tensile strength of the lap joint is higher than 178 MPa (the joint area: ca. 80 mm²). As previously reported, the tensile or shear tensile specimens frequently fracture at the interface of the dissimilar joint because of the formations of intermetallic compound layers [1–4,7–9], and thus the tensile strength is comparatively low. In the present work, the lap joint has a considerably high shear tensile strength, so that specimens broke at the base metal. The high strength of the lap joint can be supposed to result from the microstructures of the lap joint interface, where tiny Fe–Ti intermetallic particles are dispersed and mixed with β titanium in layers. It should be pointed out, however, that the wear of tool is comparatively severe in the present work, and tools made from more

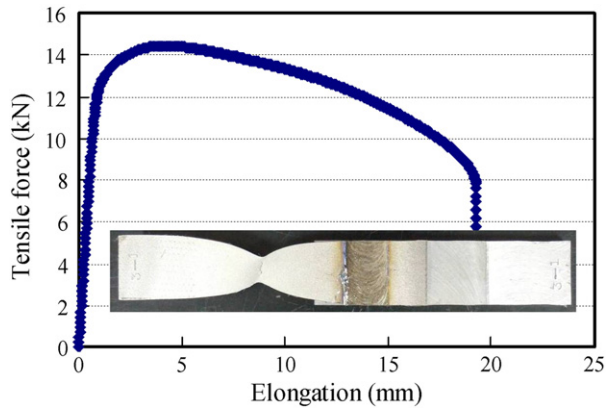


Fig. 4. Force–elongation curve and fracture location of shear tensile test of the lap joint.

advanced materials such as PCBN [10] are required for practical welding.

4. Conclusion

A commercially pure titanium plate was lap-joined to a structural steel plate via friction stir welding, and the microstructures at the lap

joint interface were intensively examined by EBSD and TEM. Swirling-like macro- and micro-intermixing zones are formed at the joint interface. At the macro-intermixing zones, α titanium and steel are mixed in swirling morphology; at the micro-intermixing zones, the tiny Fe–Ti intermetallic particles are dispersed and mixed with β titanium in layers, and in the area adjacent to the micro-intermixing zone, the grain size of titanium and steel becomes very small. The high tensile strength of the lap joint is supposed to be attributed to the microstructures at the joint interface.

References

- [1] Ghosh M, Kundu S, Chatterjee S, Mishra B. *Metall Mater Trans A* 2005;36:1891–9.
- [2] Kundu S, Chatterjee S. *Mater Sci Eng A* 2007;480:316–22.
- [3] Elrefaey A, Tillmann W. *J Mater Process Technol* 2009;209:2746–52.
- [4] Kundu S, Chatterjee S. *Mater Sci Eng A* 2006;425:107–13.
- [5] Meshram SD, Mohandas T, Madhusudhan Reddy G. *J Mater Process Technol* 2007;184:330–7.
- [6] Kostka A, Coelho RS, Dos Santos J, Pyzalla AR. *Scr Mater* 2009;60:953–6.
- [7] Yamamoto N, Liao J, Watanabe S, Nakata K. *Mater Trans* 2009;50:2833–8.
- [8] Chen Y, Nakata K. *Scr Mater* 2008;58:433–6.
- [9] Tanaka T, Morishige T, Hirata T. *Scr Mater* 2009;61:756–9.
- [10] Mironov S, Sato YS, Kokawa H. *Acta Mater* 2009;57:4519–28.
- [11] Cui L, Fujii H, Tsuji N, Nogi K. *Scr Mater* 2007;56:637–40.
- [12] Villars P, Prince A, Okamoto H. *Handbook of ternary phase alloys*, 7. Materials Park, OH: ASTM Inter.; 1995. p. 8903–28.
- [13] Knipling KE, Fonda RW. *Scr Mater* 2009;60:1097–100.
- [14] Liao J, Yamamoto N, Nakata K. *Metall Mater Trans* 2009;40A:2212–9.